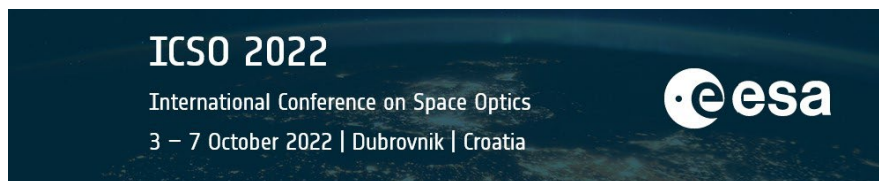


# International Conference on Space Optics—ICSO 2022

Dubrovnik, Croatia

3–7 October 2022

*Edited by Kyriaki Minoglou, Nikos Karafolas, and Bruno Cugny,*



## *Photonic Integration and Integrated Microwave Photonic Technologies for Satellite Applications*



---

# Photonic Integration and Integrated Microwave Photonic Technologies for Satellite Applications

Hakimeh Mohammadhosseini<sup>\*a</sup>, Stephan Roemer<sup>a</sup>, Pierre Darmon<sup>a</sup>, Ness Schelkens<sup>a</sup>, Durvasa Gupta<sup>b</sup>, Klemens Janiak<sup>b</sup>, Gerrit Fiol<sup>b</sup>, Jeong Hwan Song<sup>c</sup>, Roelof Jansen<sup>c</sup>, Grahame Wood<sup>d</sup>

<sup>a</sup>Antwerp Space, Berkenrodelei 33, 2660 Antwerpen, Belgium

<sup>b</sup>Fraunhofer Heinrich Hertz Institute, Einsteinufer 37, 10587 Berlin, Germany

<sup>c</sup>IMEC, Kapeldreef 75, Leuven, 3001, Belgium

<sup>d</sup>Alter Technology TÜV Nord UK Ltd, UK

\*hakimeh.mohammadhosseini@antwerpspace.be

## ABSTRACT

Inter-satellite communication links and laser communication terminals face challenges that could be solved with new photonics technologies i.e., photonic integrated circuits (PIC) and integrated microwave photonics. In general, these challenges are the need for higher data-rate, and reduced Size, Weight and Power Consumption (SWaP). In this paper we present the potential of integrated microwave photonics for intra-satellite communication links and photonic integration for laser communication terminals by demonstrating latest progress of Antwerp Space Q/V-band Electro-Photonic Frequency Converter (EPFCV2) and Photonic Lantern Receiver (PLR).

**Keywords:** Photonic Integration, Integrated Microwave Photonics, Silicon photonics, Intra-satellite links, Laser Communication Terminals

## 1. INTRODUCTION

Photonic Integration Technology & in particular Integrated Microwave Photonics (iMWP) Technology [1] can offer a significant advantage over classical RF solutions for intra-satellite communication links [2]. Intra-satellite communication requirements such as Terabit/s data rate, insensitivity to Electromagnetic Interference (EMI), low volume, low mass, low power consumption, as well as ease of Assembly, Integration, and Test (AIT), are key drivers of the need for optical communication, e.g. inside the satellite [3]. Comparing to classical RF solutions, the main benefits of photonics technology comes along when going to higher frequency regimes e.g., Q, V, and W frequency bands, and when ultra-low loss signal transmission, with mechanical flexibility, is required for instance inside a communication satellite. Benefits of photonics technology is not limited to intra-satellite links but can be extended to laser communication terminals (LCTs) as well. There is a great need for a non-mechanical, compact, low-loss, low-cost solution in the receiving side of LCTs. A PIC-based solution can be used to replace the classical mechanical fine pointing assembly (FPA) of the LCTs as a pure non-mechanical solution. Comparing to state-of-the-art technologies, a PIC-based lantern receiver offers advantages like large receiving area and possibility of eliminating the FPA, integrating APD-Photo-detection, and 4Q sensor functionality on the same platform.

In this paper we present latest results of EPFCV2 and PLR. In Section 2, we briefly present Antwerp Space Q/V band EPFCV2 module and discuss technical specification and fabrication/simulation results, both on package level and PIC level. In section 3, we present the PLR project. We discuss the need for a PIC-based solution inside LCT terminals and main technical specifications as well as our verification strategy. We then show latest fabrication and simulation results on PIC level. Finally initial schematic of the control board is presented.

EPFCV2 is a funded project by ESA under ARTES C&G program. PLR is a funded project by ESA under ARTES AT 5C.392.

Antwerp Space partners for EPFCV2 project are Alter (UK) and Fraunhofer Heinrich Hertz Institute (DE). For Photonic Lantern project we collaborated with IMEC (BE) and Mynaric (DE).

## 2. INTEGRATED MICROWAVE PHOTONICS FOR INTRA-SATELLITE COMMUNICATION LINKS

In this section we present latest advancement of Antwerp Space Q/V-band EPFCV2. Firstly, we demonstrate the mechanical assembly of EPFCV2 module and the position of the hermetically

Packaged Photonic Integrated Circuit (PPIC) inside this module. Secondly, we present the PIC and PPIC requirements in more detail. Finally main measurement results on the PIC level are presented.

### 2.1 Antwerp Space EPFCV2: A Q/V band Electro-Photonic Frequency Convertor Module

Figure 2-1 presents AWS Q/V band frequency convertor design. The golden box inside the module is the PPIC. A specific electronic design is made to control PIC components inside the gold box. A Q/V band LNA is integrated to compensate for the optical insertion losses. Polarization maintaining fibers are attached to the output and input of Tx & Rx PICs, respectively. The fiber optic connection to Tx and Rx dies not only enable RF-over-Fiber distribution but also provide the possibility to add an extra amplification stage between Tx and Rx dies. Positioning an amplification stage between the Tx and Rx PICs is a risk mitigation approach in case of high optical insertion losses or low out power of integrated DFB laser.

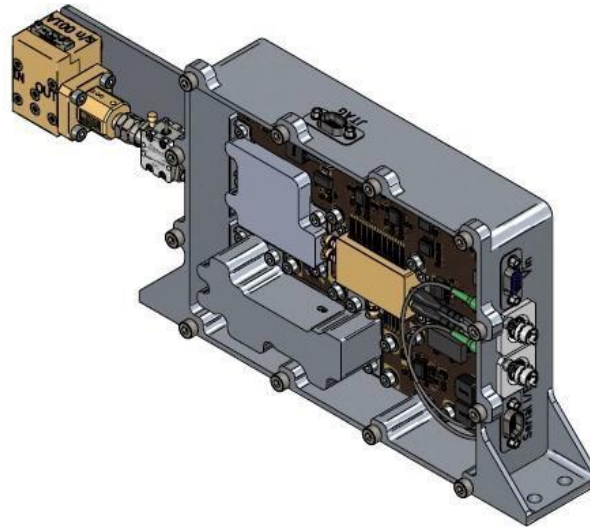


Figure 2-1 Antwerp Space Q/V band Frequency Convertor Module. The gold package inside the module is the PPIC. One of the optical fibers is connected to the Tx while the other enable the optical connection to the Rx.

Table 2-1 EPFCV2 Technical specification

Specification	Value	Unit
Operational RF Frequency Range	47.2 to 50.2	GHz
LO Frequency	30	GHz
IF Frequency	17.2 to 20.2	GHz
F-conversion Technology	Photonic Integration	NA
Operational optical wavelength	C-band	nm
Optical Interface	Mini AVIM	NA
RF, LO, and IF inputs	Feedthrough pins	NA
RF input power range	-60 to -35	dBm

### 2.2 EPFCV2 packaging requirements: A Hermetically Sealed Space Qualified PIC

A hermetically sealed space-qualified package was developed during EPFCV2 project which is shown in Figure 2-2. The package contains Tx and Rx dies, Thermal Control element (TEC) and an optical bench. Although Tx and Rx are

separate dies they are placed inside a single package and use a single TEC (for SWaP reduction). All materials and joints developed for this product are space qualified and has followed space qualified packaging methods & techniques<sup>1</sup>. Main technical specifications of PPIC is presented in Table 2-2.

To ensure PPIC is robust w.r.t stresses caused by thermal loading, contraction or expansion various design and simulations have been performed to ensure desired thermal, RF, and optical performance. For thermal performance design, thermal simulations have been done on PPIC and on different join levels, i.e., TEC to package, TEC to optical bench, etc. Based on thermal simulation results this package meet a great mechanical integrity when PPIC temperature range is set between -65°C to +15°C. On the PPIC RF performance, three discrete RF circuits, i.e., 50 GHz RF, 30 GHz LO, and 20 GHz IF have been designed starting from their connector down to connections to the PIC interfaces. Target metrics were 50 Ohm impedance, <0.5 dB insertion loss, and <20 dB return loss.

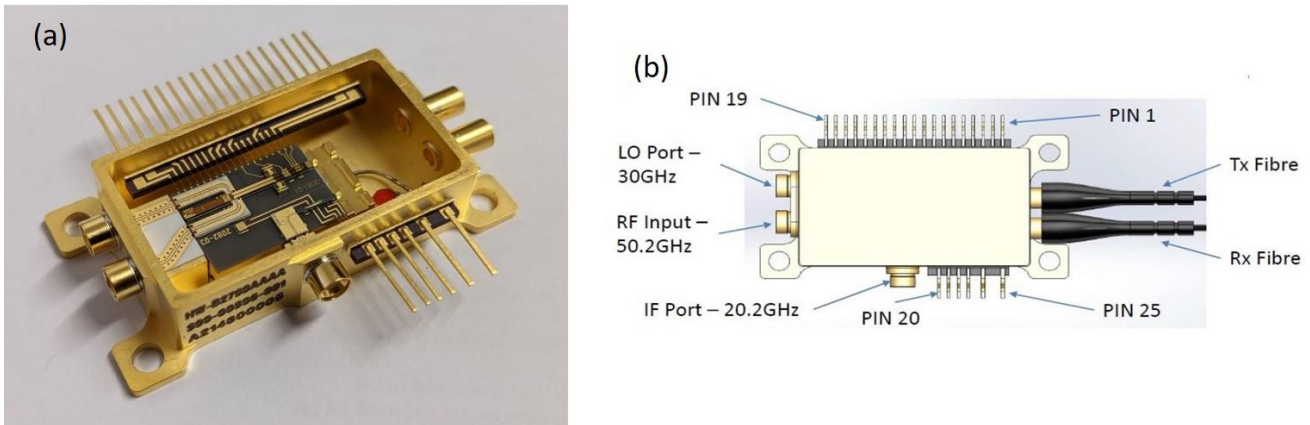


Figure 2-2 (a) PPIC assembly without lid (by Alter UK) (b) Hermetically sealed PIC-based electro-photonic frequency converter: DC pins are designed to DC bias PIC components inside the package, Optical Fibers are attached to TX and Rx PICs. : The PPIC assembly is designed and fabricated by Alter UK.

On PPIC optical performance, coupling efficiency of fibers to the optical chips both on Tx and Rx sides have been evaluated. Optical modelling showed 73% and 80% coupling efficiency for Tx and Rx, respectively.

Table 2-2 PPIC Technical Specifications

Specification	Value	Unit
PPIC size <sup>2</sup>	40 × 26 × 16	mm <sup>3</sup>
PPIC mass	<40	grams
PPIC components	Thermal, Optical, and RF parts	NA
Material and Processes of PPIC are in accordance with ECSS-Q-ST-70C		

We have now presented the EPFCV2 module as well as PPIC position and details. In the next section, we focus on the integrated microwave photonic link inside the PPIC following by measurement results on each of Tx/Rx dies.

### 2.3 EPFCV2 Tx/Rx PIC: An integrated Microwave Photonic link

Figure 2-3 shows the microwave photonic link (with integrated Tx and Rx dies) which is the baseline of the frequency down-conversion in EPFCV2 project. On the Tx side, a DFB laser is integrated with a high-speed IQM modulator on InP photonic integration platform and on the Rx side an SOA is integrated with a high-speed PD. Spot Size Converters (SSC) are considered for coupling the light outside the Tx PIC and inside the Rx PIC, respectively. Space-qualified Mini

<sup>1</sup> There are few exceptions to this. For example because there are no Thermo-electric coolers on ESA QPL, a TEC is considered for this package with a construction which is as close as possible to a space-qualified product.

<sup>2</sup> Including DC pins and mounting flanges

AVIM connectors are used on both Tx and Rx together with a single-mode polarization maintaining optical fiber. TEC's are foreseen on both Tx and Rx side in order to keep the PIC temperature at 20°C.

In theory there are multiple photonics-based approaches for frequency down-conversion like a mode-locked laser integrated with a Mach-Zehnder modulator [4], an integrated dual-polarization dual-parallel MZM with tunable optoelectronic oscillator (OEO) and phase shift [5] or a dual-drive MZM [6]. In our case we considered an IQM which has two child-MZMs in each arm. This design enables us to apply RF and LO signals on each arm of IQM while at the same time gives the flexibility to DC bias either each of the IQM arms or child-MZMs.

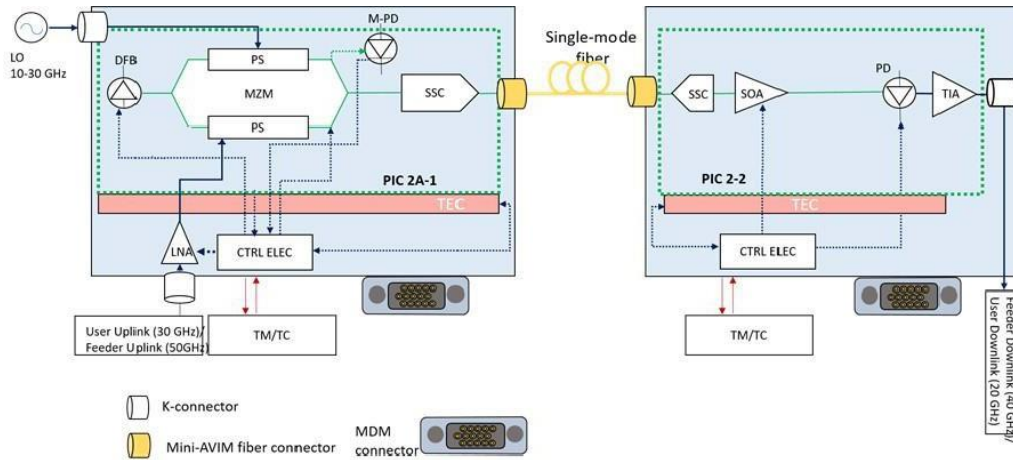


Figure 2-3 A Microwave photonic link with integrated Tx and Rx photonic chips as a baseline technology of EPFCV2 frequency down-conversion. A DFB laser is integrated with a high-speed IQM on Tx side. On the Rx side an SOA is integrated with a high-speed Photo-detector (PD). SSC stands for Spot Size convertor. TIA could be integrated into the PD or placed outside of the PIC.

We summarize this section by presenting the main design metrics of Tx/Rx dies in Table 2-3 and a general view on Tx/Rx layouts in Figure 2-4.

Table 2-3 Main technical specifications of EPFCV2 Tx/Rx dies.

Metric	Value	Unit
IQM modulator 3dB Bandwidth	50	GHz
Wavelength range	C-band	nm
Laser type	DFB	NA
Laser RIN	<140	dB/Hz
Laser linewidth	< 3	MHz
SMSR	40	dB
PD 3dB BW	<20	GHz
PD responsivity	0.8	A/W
SOA Gain	20	dB

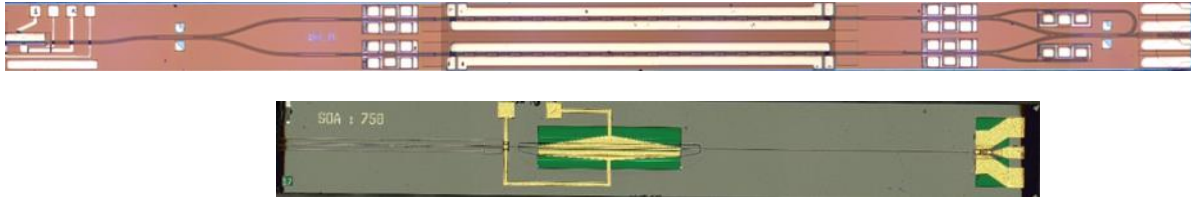


Figure 2-4 Laser integrated with IQM on Tx side (top) and SOA integrated with PD on Rx side (bottom).

## 2.4 Tx/Rx Main Measurement Results

In this section we present main finding of measurements from Tx and Rx dies. On Tx, laser characteristics have been measured by the foundry (HHI, DE) the result of which is shown in Figure 2-5. These results are in accordance with specified metrics in Table 2-3. The 3dB electro-optic response of IQM is shown in Figure 2-6. As it is shown, there is a slight difference with the intended 50.2 GHz 3dB bandwidth. It has to be noted that this value corresponds to both child-MZMs in IQM design.

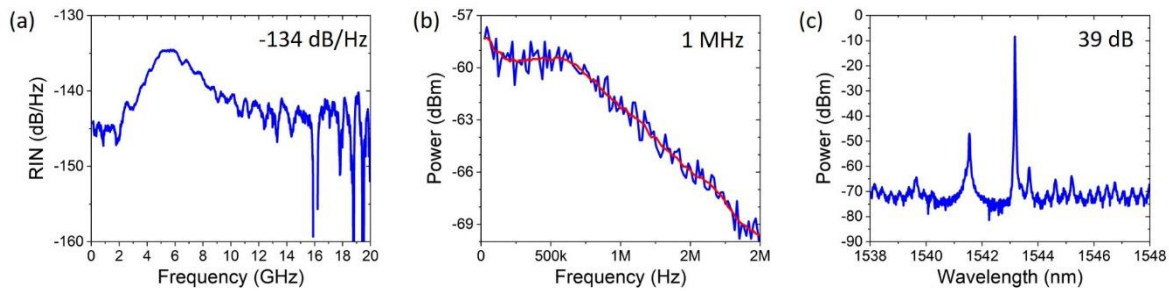


Figure 2-5 Measurement results of laser characteristics at 110 mA of laser current (a) RIN, (b) linewidth (blue curve as measured, red 10 pts adjacent average) and (c) SMSR

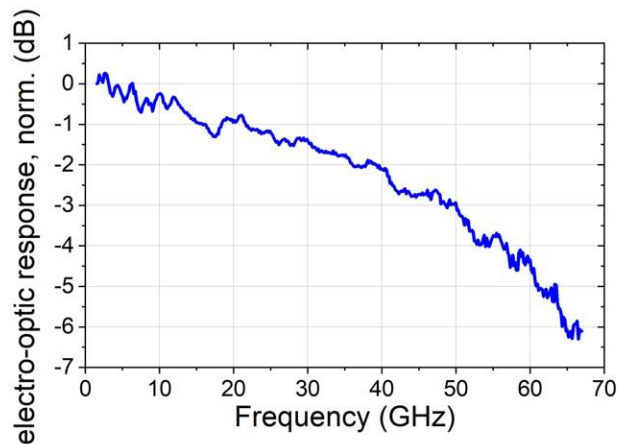


Figure 2-6 Measured 48.6 GHz 3dB electro-optic response of the IQM modulator on Tx die

On the Rx side a 36.5 GHz bandwidth has been measured for the photo-detector. On the same wafer run and design, the integrated SOA showed larger than 20dB of gain. The details of these results are shown in Figure 2-7.

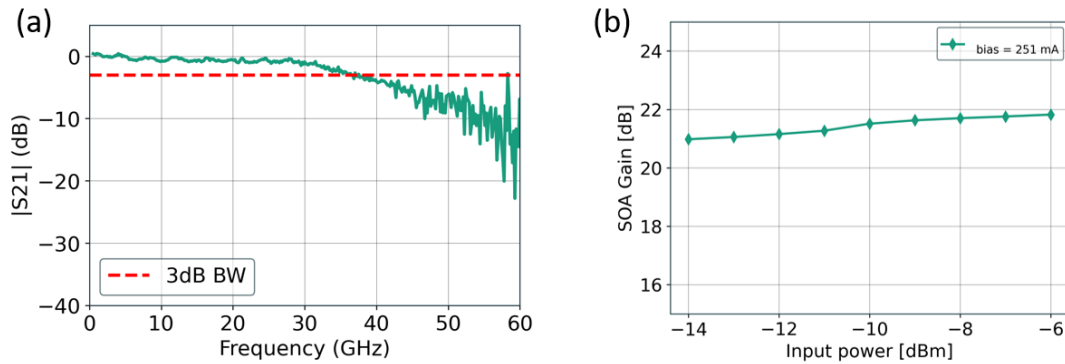


Figure 2-7 Measured (a) 36.5 GHz 3dB bandwidth of the photo-diode on Rx dies and (b) SOA Gain on Rx dies. This measurement comes from the same wafer run.

Responsivity of PDs on the same wafer run showed a good compliance to specification of 0.8 A/W as shown in Figure 2-8.

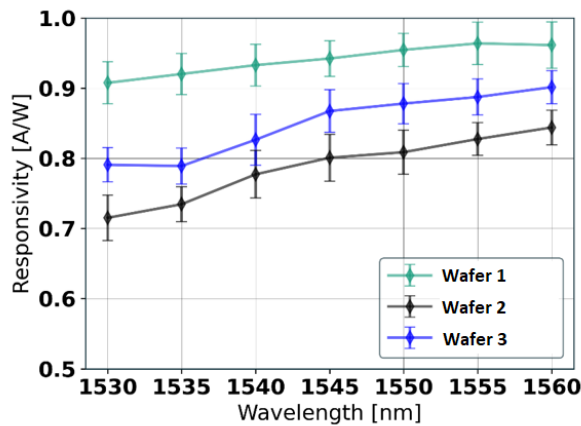


Figure 2-8 Measured responsivity of photodiodes on 3 different HHI wafers

Once the PICs are integrated into the final packaging assembly the system metrics like Gain, NF, SFDR, and power consumption will be measured.

### 3. PHOTONIC INTEGRATION TECHNOLOGY FOR LASER COMMUNICATION TERMINALS

In this section we present the latest results of Photonic Lantern Receiver (PLR) project. The objective of this project was to develop, manufacture and test a Breadboard Model of a PLR. Different technologies are available for fabrication of PLR which are Multi-Plane Light Conversion (MPLC) technology [7], Optical fiber technology [8], and Photonic Integration technology. While MPLC technology has a high reliability due to its passive nature, the mechanical requirements are very challenging to meet using this approach, since a submicron positioning accuracy is required for the

free-space components. For an integration inside a laser communication terminal, Assembly, Integration and Test (AIT) is challenging as well since functionalities like 4Q sensor, and Photo-detection need to be integrated with the PLR. This will in turn increase the recurring cost of the PLR to be used inside LCT terminals.

Optical fiber technology based lantern have a good reliability due to its passive nature while for its application inside LCTs, AIT is challenging because it only provides lantern solution and not the required 4Q sensor and photo-detection. Photonic integration technology [9] based PLR could solve these challenges because it provides not only a lantern solution which can extends in terms surface area (in principle till wafer dimension) but also brings along an integrated photo-detector. Therefore AIT is excellent for PIC-based lantern as there is no need for a dedicated 4Q sensor, or photo- detection inside the LCT terminals. Therefore we developed the PLR based on photonic integration technology the details of which is presented in the next sections.

### 3.1 Antwerp Space PIC-based Photonic Lantern Receiver

The PIC-based PLR is designed to solve main challenges of current LCT terminals. Important LCT requirements are: I) increasing the surface of receiving area, II) integration of a non-mechanical solution with the photo-detector, III) high data rate, and IV) reduced AIT & cost. We present main design metrics and technical specifications of the Antwerp Space PIC-based lantern in Table 3-1.

Table 3-1 Main technical specifications of PIC-based PLR

Metric	Value	Unit
Receiving area	200 × 200	μm <sup>2</sup>
Optical insertion losses	-10.5	dB
Operating wavelength	1550	Nm
Data rate	1.2	Gbps
PD responsivity	0.8	A/W
Rx input requirement	Single Optical input	NA
Rx output channel	Single signal output	NA
Features	Non-mechanical, with an integrated PD, 4Q sensor, extendable surface area	

PLR hardware and test strategy is presented in Figure 3-1. As it can be seen, a PIC-based lantern is positioned on a Thorlab cage system to enable proper positioning of incoming laser light converged using an optical lens system. The Photo-diodes on PIC are wire-bonded to Trans-Impedance Amplifiers (TIAs) to amplify the signal. A dedicated control board is designed to enable the 4Q-sensor functionality and to transmit the electrical signals to BER tester.

This experiment is design to simulate auto-detection of incoming laser light on a PLR receiver inside a LCT terminal. The idea is to steer the laser light over the PLR receiving area which is 200μm × 200μm and to automatically detect it at BER tester using the 4Q sensor approach and at 1.2 Gbps data-rate. In the next sections we present design and characterization of the main receiving components inside the PIC i.e., GCs and PDs.



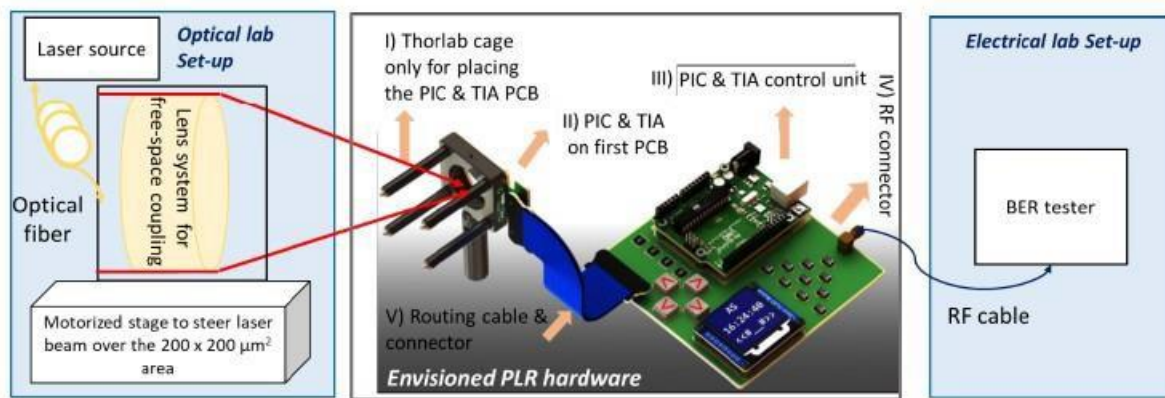


Figure 3-1 Envisioned PLR hardware and test strategy.

### 3.2 Grating Couplers: Passive Receiving components for PIC-based PLR

The PLRPIC-based approach is a non-mechanical solution which is based on passive Grating Coupler (GC) arrays. GC arrays ( $14 \times 12$ ) are designed in an end-fire/back-fire approach covering an area of  $200\mu\text{m} \times 200\mu\text{m}$ , as presented in Figure 3-2. The incident angle of incoming laser light is  $10^\circ$  which is typical for silicon photonics [10]. Each of these GCs are connected via optical waveguide to a single PD with a responsivity better than  $0.8 \text{ A/W}$  and a bandwidth larger than  $5 \text{ GHz}$ . The PICs are designed and fabricated at IMEC (BE) and on IMEC silicon photonics platform.

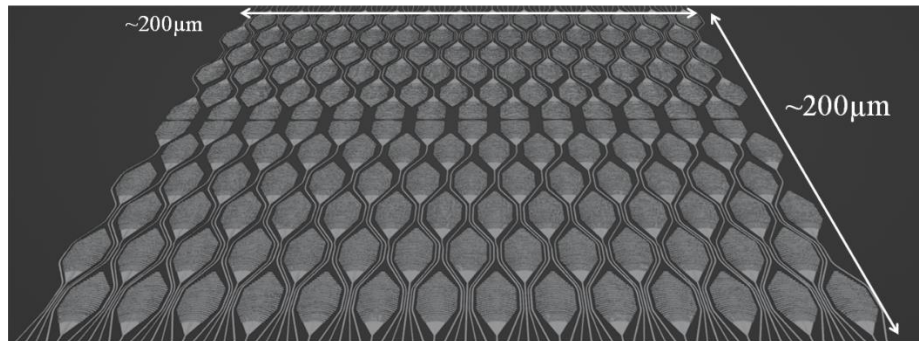


Figure 3-2 Grating couplers covering an area of  $200\mu\text{m} \times 200\mu\text{m}$  in an end-fire back-fire design configuration (by IMEC) [11].

Coupling efficiencies of GCs are calculated using both a  $10 \mu\text{m}$  source and a  $20 \mu\text{m}$  source and is shown in Figure 3-3. The  $10 \mu\text{m}$  source is used at early test stage because it was available at IMEC, while the  $20 \mu\text{m}$  source will be used later during testing of the PLR.

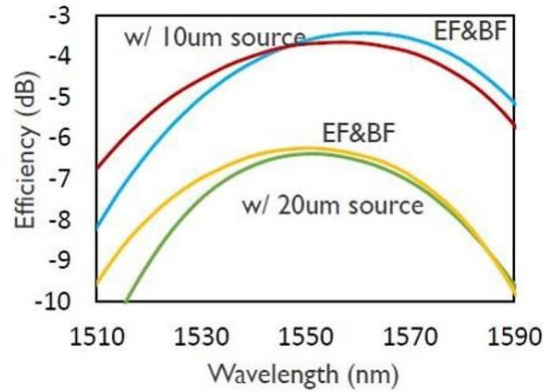


Figure 3-3 Calculated coupling efficiencies of end-fire (EF) and back-fire (BF) Grating Couplers (GC) (by IMEC) [11].

Coupling efficiencies of the fabricated PICs have been calculated not only on single GCs but also over the whole chip surface area. The simulation results for a 10  $\mu\text{m}$  and a 20  $\mu\text{m}$  source are shown in Figure 3-4. For a larger mode-field diameter of 20  $\mu\text{m}$  the simulation results which is presented in Figure 3-4 (b) shows higher coupling efficiency of minimum 10.5 dB for 95% of the whole receiving area [11]. It should be noted here that the PDs are also measured at IMEC and have shown responsivity of larger than 1.1 A/W for reverse biased ranging from -1 V to -3 V. These results are in accordance with technical specification of PIC-based PLR which was previously presented in Table 3-1.

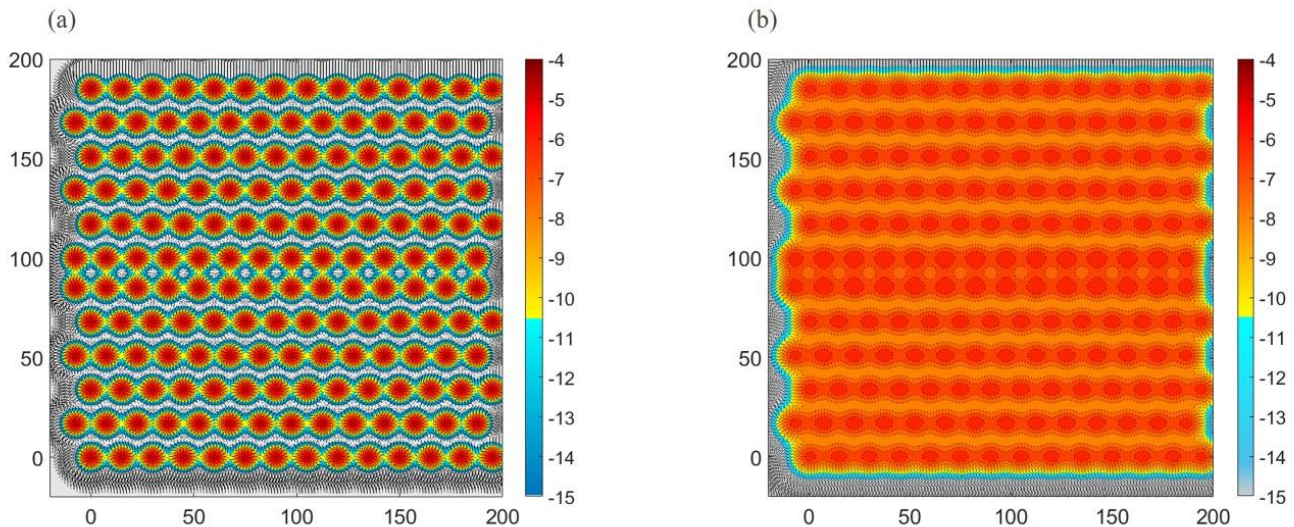


Figure 3-4 Simulation results of coupling efficiency over  $200\mu\text{m} \times 200\mu\text{m}$  design area for a  $14 \times 12$  array using (a)  $10\mu\text{m}$  diameter source and (b) using a  $20\mu\text{m}$  diameter source [11].

### 3.3 Control electronics for PIC-based PLR

The control electronics for the PIC-based lantern also enables the 4Q sensor functionality. The initial schematic of the design is shown in Figure 3-5. Each quadrant of the PIC is connected to a single TIA via the PDs. Later each TIA will be wire-bonded to a total number of 42 PDs. The microcontroller enables switching functionality and the board has a single output for BER measurement purposes.

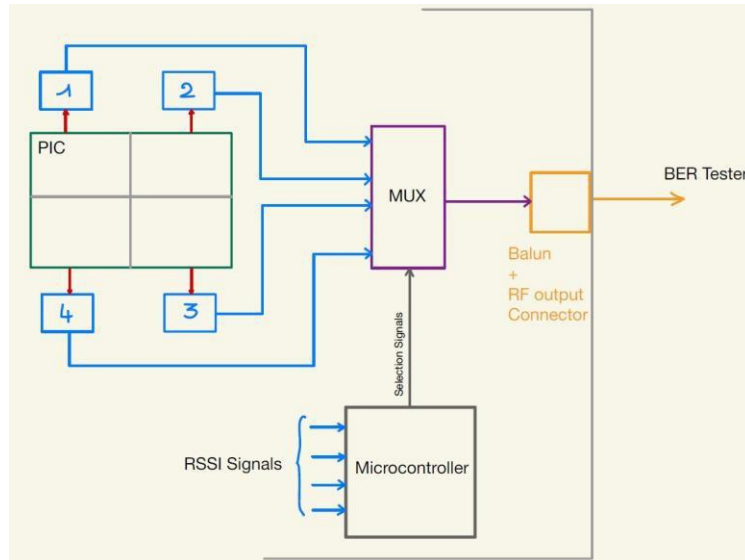


Figure 3-5 Initial schematic of the control electronics for photonic lantern receiver. A 4Q sensor functionality is envisioned for automatic detection of laser light while sweeping over the area of  $200\ \mu\text{m} \times 200\ \mu\text{m}$ .

#### 4. CONCLUSION & OUTLOOK

We presented Antwerp Space’s EPFCV2 and Photonic Lantern projects, which are both funded by ESA in the ARTES program. EPFCV2 shows the benefits of integrated microwave photonics for satellite application, e.g. Q/V-band to K-band frequency high-bandwidth down-conversion, RF-over-Fiber application, and reduction of AIT efforts inside telecom payloads. The Photonic lantern project presents importance of photonic integration technology inside a cost effective, and mass producible, laser communication terminals. This project is a proof-of-concept showing the role of PIC technology for solving current challenges of LCT terminals. PIC-based LCT provides benefits such as large receiving area, integrated photo-detection, and as a result reduced AIT, and cost. Therefore Antwerp Space plans the development of on-board space communication equipment based on this technology.

Equipment using EPFCV2 technology will focus on improved performance of PIC in terms of output power and noise figure either through PIC design or hybrid integration platform. Hybrid PIC integration platforms provide best of both worlds in terms of output power, noise figure, and insertion losses. Another improvement is foreseen for reducing the total power consumption by eliminating the TEC, because of low efficiency of TECs. For the photonic lantern project, we foresee improvement in terms of optical insertion losses. This requires either improvement via GC design and/or using a double integration layer for increasing the number of GCs and therefore increasing the fill factor significantly. In terms of control electronics, the next generation of PIC-based PLR would use FPGAs (based on our on board processing hardware heritage) instead of switches for a fast detection of laser signals and higher integration/lower mass & volume.

#### 5. ACKNOWLEDGEMENT

We would like to thank ESA and BELPSO for supporting AntwerpSpace with ARTES funding of the EPFCV2 and Photonic Lantern projects. We also thank all are partners in EPFCV2: Alter (UK) and HHI (DE) and in Photonic Lantern: IMEC (BE) and Mynaric (DE).ssss

#### REFERENCES

- [1] D. Marpaung, et al, “Integrated Microwave Photonics” Laser & Photonics Reviews, Rev. 0, No. 0, 2012.
- [2] J. Anzalchi, Final Demonstration Results of OPTIMA, Photonic Payload for Telecommunication Satellites, International Conference on Space Optics (ICSO 2020).

- [3] K. Balakier, Integrated Photonics for Wireless and Satellite Applications, Advanced Photonics congress, OSA 2020.
- [4] K. Van Gasse, et al, “Ka-to-L-band frequency down-conversion using a micro-photonic III-V-on-silicon mode-locked laser and Mach-Zehnder modulator”, International Conference on Space Optics, France, 2016.
- [5] F. Yang, et al, “Photonics-assisted frequency up/down conversion with tunable OEO and phase shift”, IEEE Journal of Lightwave Technology, Vol. 38, No. 23, December 2020.
- [6] T. Jian, et al, “Microwave photonic phase-tunable mixer”, Optics Express, Vol. 25, No.4, Feb 2017.
- [7] G. Labroille, et al, “Efficient and mode selective spatial model multiplexer based on multi-plane light conversion”, Optics Express, Vol. 22, No. 13, 2014.
- [8] T. A. Birks, et al, “The Photonic Lantern”, Advances in Optics and Photonics, Vol. 7, no. 2, 2015.
- [9] J. K. Doyle and A. P. Knights, “The evolution of silicon photonics as an enabling technology for optical interconnection,” Laser Photon. Rev., vol. 6, no. 4, pp. 504–525, Jul. 2012.
- [10] S. Kumar Selvaraja, et al, “Highly efficient grating coupler between optical fiber and silicon photonic circuit”, 2009 Conference on Lasers and electro-Optics and 2009 Conference on Quantum electronics and Laser Science.
- [11] J. H. Song, T.D. Kongnyuy, M. Prost, and R. Jansen; IMEC, Leuven, Belgium and H. Mohammadhosseini; Antwerp Space, Antwerpen, Belgium, are preparing a manuscript to be called “Silicon photonic lantern receiver for satellite laser communication terminals.” September 2022.